Closing the Light Gluino Window Using $\pi^+\pi^-$ Pairs Produced in a Neutral Beam.

Amitabh Lath*

Rutgers University, Piscataway NJ 08855

We have performed an extensive search for spontaneous appearance for $\pi^+\pi^-$ pairs in a neutral beam, for invariant masses of the charged pions as low as the kinematic limit of $2M_\pi$. The main source of events with two charged particles are decays of neutral kaons, and detailed understanding of the resultant invariant mass shape constrains most hypothetical processes that produce a charged pion pair and an unobservable particle. In particular, we place a limit on the decay $R^0 \to \pi^+\pi^-\tilde{\gamma}$ for any $M_{R^0} - M_{\tilde{\gamma}} \geq 2M_\pi$. In the most interesting R^0 mass range, ≤ 3 GeV/c^2, we can exclude lifetimes from 5×10^{-10} seconds to as high as 10^{-4} seconds.

1 Introduction

Several theories of supersymmetry, including those which solve the SUSY-CP problem by eliminating dimension 3 operators [1], predict light gauginos and heavy squarks. In such theories, the super-partners of the massless bosons remain light. In fact, light masses for gluinos($\tilde{g}$) and photinos($\tilde{\gamma}$) arise naturally in many SUSY models, but have been ignored without adequate evidence for their exclusion. In most such models, the gluino and photino masses are expected to be ≤ 1.0 GeV/c^2. The gluino should form bound states with normal quarks and gluons (g), the lightest of which is called the R^0, a spin $\frac{1}{2}$ $g\tilde{g}$ bound state.

Estimates of the mass and lifetime of the R^0 vary from 1 to 3 GeV/c^2 and 10^{-10} to 10^{-5} s respectively [2]. The ratio of masses $M_{R^0}/M_{\tilde{\gamma}} \equiv$ r is expected to be $1.3 \leq r \leq 1.8$, based on particle physics [2], and cosmological [3] arguments.

1.1 Previous Searches

A previous direct search for the R^0 by this collaboration is described in [4]. That result, based on 5% of the data collected by KTeV in 1996, excluded the R^0 with the constraint $M_{R^0} - M\tilde{\gamma} \geq 0.648$ GeV/c^2. However, that previous KTeV result, along with several related indirect searches, [5][6][7][8], failed to exclude the R^0 at the required level of sensitivity in the region of primary interest, $r \leq 1.4$ [9].

1.2 R^0 Production and Decay

R^0 production in pN collisions has been discussed in [4]. It is important to note that the production may proceed through conventional QCD [11]. A light R^0 can therefore be produced in large numbers in pN collisions. The R^0 is expected to decay mainly into $\rho\tilde{\gamma}$, but may decay into $\eta\tilde{\gamma}$ or $\pi^0\tilde{\gamma}$ if C-parity were to be violated. A neutral beam fixed target experiment with a large decay volume downstream of the target is therefore the ideal place to conduct a search for the R^0. In this analysis, we concentrate on the dominant decay, $R^0 \to \rho\tilde{\gamma}$, $\rho \to \pi^+\pi^-$, in which the $\tilde{\gamma}$ escapes undetected.

2 The KTeV Experiment

The KTeV experiment is described in [10], and as used in the R^0 search in [4]. The neutral beam, extracted from a BeO target with 800 GeV/c protons incident, was allowed to propagate for approximately 100 m; then decay in a volume approximately 50 m long. The products of the decays were detected by a spectrometer consisting of four drift chambers with single-hit resolution of $\leq 100\mu$m and a 3100 element pure CSI calorimeter with electromagnetic energy resolution of $\leq 1\%$. In addition, a series of muon hodoscopes downstream of the calorimeter were used to identify tracks as muons.

3 Data Analysis

The data used in this analysis were collected during the 1996 run of KTeV (FNAL E832). The trigger and analysis cuts used are similar to those described in [4]. To detect a possible R^0 signal we examined decays with two charged particles; specifically the shape of the invariant mass distribution, with the assumption that the particles were pions ($M_{\pi^+\pi^-}$). Backgrounds consisted of $K_L \to \pi^\pm l^\mp \nu$ ($l = e, \mu$) decays with leptons misidentified as pions (semi-leptonic decays); $K_L \to \pi^+\pi^-$ and $K_L \to \pi^+\pi^-\gamma$ decays; as well as $K_L \to \pi^+\pi^-\pi^0$ decays with undetected π^0's.

Semi-leptonic decays were identified and rejected in a manner similar to that described in [4]. Tracks made by electrons were identified as such since the energy they deposited in the calorimeter matched the momentum measured by the spectrometer. Muon tracks were identified by extrapolating the track from the spectrometer to one or more hits in the muon hodoscopes. The $K_L \to \pi^+\pi^-$ decays were rejected by requiring the transverse momentum squared of the $\pi^+\pi^-$ with respect to the beam direction (P_t^2) to be greater than 0.001 (GeV/c)^2. The $K_L \to$

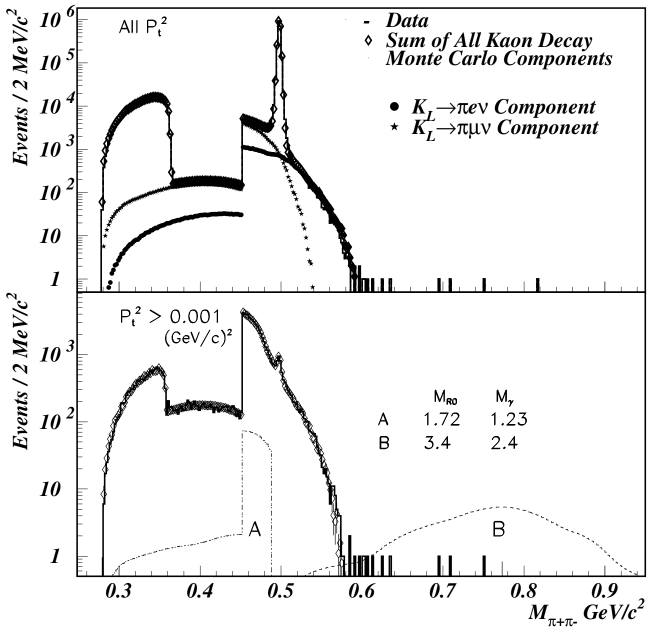

Figure 1: $M_{\pi^+\pi^-}$ distribution with all but P_t^2 and $K_L \to \pi^+\pi^-\pi^0$ specific cuts (top), and all cuts (bottom). The solid line is data, and diamonds are the sum of all kaon decay simulations. The data with $M_{\pi^+\pi^-} \leq 0.45$ GeV/c^2 is from a data stream with a trigger prescale. The contribution of $K_L \to \pi^\pm e^\mp \nu$ (dots) and $K_L \to \pi^\pm \mu^\mp \nu$ (stars) decays is also shown. In the bottom plot, the distributions due to two sample R^0's of lifetime $\tau = \tau(K_L)$, and 1/10 of the pQCD predicted flux are shown (dash, dot-dash), labelled A and B. The masses are in GeV/c^2.

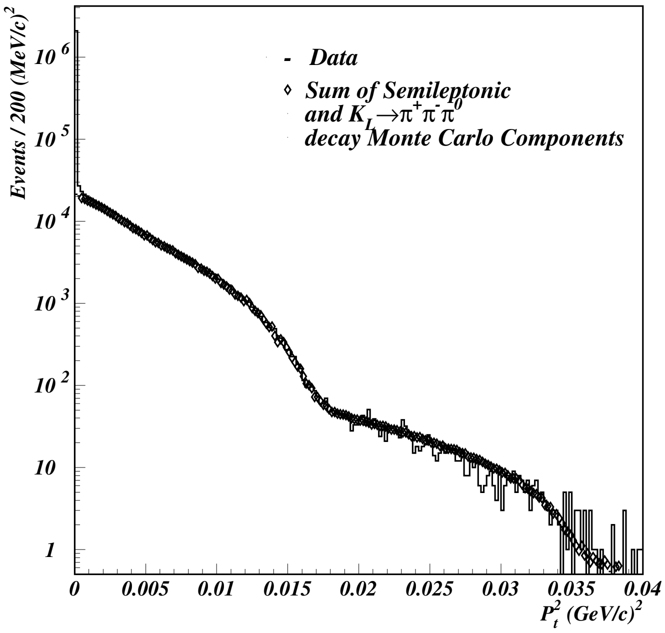

Figure 2: P_t^2 distribution for the data, with all cuts but P_t^2 and $K_L \to \pi^+\pi^-\pi^0$ specific cuts. The data (solid) has a spike at zero due to $K_L \to \pi^+\pi^-$ decays. The diamonds show the sum of the semileptonic and $K_L \to \pi^+\pi^-\pi^0$ decays.

$\pi^+\pi^-\gamma$ and $K_L \to \pi^+\pi^-\pi^0$ decays were rejected by identifying photons in the calorimeter from these decays. Additional cuts in the region $M_{\pi^+\pi^-} \leq 0.36$ GeV/c^2 on energy deposited in the calorimeter further rejected the $K_L \to \pi^+\pi^-\pi^0$ decays ($K_L \to \pi^+\pi^-\pi^0$ specific cuts).

Figure 1 (top) shows the $M_{\pi^+\pi^-}$ distribution for all the data, without the $K_L \to \pi^+\pi^-\pi^0$ specific and P_t^2 cuts. The data (solid) and the appropriately weighted sum of all K_L decay components (diamonds) are shown. The contributions of the semi-leptonic kaon decays (dots, and stars) are also shown separately. There are $\sim 2.1\times10^6$ CP-violating $K_L \to \pi^+\pi^-$ decays in the peak at M_K. An edge is evident at $M_{\pi^+\pi^-} = 0.45$ GeV/c^2. The data with $M_{\pi^+\pi^-} \leq 0.45$ GeV/c^2 is from a data stream collected with a trigger prescale, since the main charged-track data stream concentrated on $K_L \to \pi^+\pi^-$ decays, and filtered out events with $M_{\pi^+\pi^-} \leq 0.45$ GeV/c^2. The CP-conserving $K_L \to \pi^+\pi^-\pi^0$ decays are evident at $M_{\pi^+\pi^-} \leq 0.36$ GeV/c^2, and the kinematic limit is evident at $2M_\pi = 0.28$ GeV/c^2. The data and kaon decay simulation are in agreement for over six orders of magnitude.

Figure 1 (bottom) shows the $M_{\pi^+\pi^-}$ distribution for the data (solid) with all the cuts and the sum of the K_L decay simulations (diamonds) are shown. The $K_L \to \pi^+\pi^-$ peak is significantly reduced due to the P_t^2 cut, and the $K_L \to \pi^+\pi^-\pi^0$ specific cuts reduce the number of events at $M_{\pi^+\pi^-} \leq 0.36$ GeV/c^2. Two sample R^0 distributions are shown (dash, dot-dash), to illustrate their effect on the $M_{\pi^+\pi^-}$ distribution. The masses of the sample R^0 shown are 1.72 and 3.4 GeV/c^2, and the respective photino masses are 1.23 and 2.4 GeV/c^2, for the distributions labelled A and B. The number of the sample R^0 in the distributions is set at $1/10^{\text{th}}$ of that expected due to the flux predicted by perterbative QCD (pQCD) [11][12], at a lifetime equal to that of the K_L.

In the data, there are 12 events with $M_{\pi^+\pi^-} \geq 0.6$ GeV/c^2 that are not simulated by K_L decays. The number of events is consistent with that expected from interactions of the beam with residual gas in the vacuum decay volume. The sample R^0 distributions shown in figure 1 illustrate the effect of $R^0 \to \pi^+\pi^-\tilde{\gamma}$ decay on the $M_{\pi^+\pi^-}$ shape. Since the shape due to R^0 decay is significantly different from those due to kaon decays, we can

Table 1: Results for various R^0, $\tilde{\gamma}$ combinations from the MINUIT fit. The first two columns are the R^0, $\tilde{\gamma}$ masses; the third column is the 90% C.L. upper limit for the number of R^0 decays found in the data; the fourth column is the 90% C.L. upper limit for the number of R^0 produced at the target (for $\tau = \tau(K_L)$). The fifth and sixth columns are the 90% confidence level upper limit for the R^0/K^0 flux at the target, and the prediction for this flux ratio using pQCD.

$\mathbf{M_{R^0}}$ GeV/c^2	$\mathbf{M_{\tilde{\gamma}}}$ GeV/c^2	**Observed (90% C.L. Limit)**	**Produced (90% C.L. Limit)**	**R^0/K^0 Flux**	**Expected Flux (pQCD)**
3.40	2.40	13.7	50×10^3	1.3×10^{-7}	5.2×10^{-5}
1.72	1.23	929.8	7.2×10^6	1.9×10^{-5}	2.1×10^{-3}
1.61	1.15	455.8	13×10^6	3.5×10^{-5}	2.7×10^{-3}
1.16	0.83	78.5	4.6×10^6	1.2×10^{-5}	6.6×10^{-3}
1.07	0.69	236.7	11.9×10^6	3.2×10^{-5}	8.74×10^{-3}
0.93	0.60	76.0	4.1×10^6	1.1×10^{-5}	11.9×10^{-3}
0.55	0.25	23.1	2.5×10^6	6.7×10^{-6}	27.4×10^{-3}

conduct a search for the R^0 by inspecting the $M_{\pi^+\pi^-}$ shape and its difference from that expected from summing the $M_{\pi^+\pi^-}$ shape from the various kaon decays. The data shows no deviation in the $M_{\pi^+\pi^-}$ shape that could indicate a contribution from an R^0 decay. Quantitative limits on R^0 were obtained from a maximum likelihood fit explained below.

Figure 2 shows the P_t^2 distribution for all the data. The CP violating $K_L \to \pi^+\pi^-$ events are evident in the first bin, which covers the range 0 to 200 (MeV/c)^2. The solid distribution is the data, while the diamonds are the sum of the semileptonic and $K_L \to \pi^+\pi^-\pi^0$ decay Monte Carlo simulations. The data at higher P_t^2 is well matched by a combination of semileptonic and $K_L \to \pi^+\pi^-\pi^0$ decays. The magnitudes for the kaon decay components were fixed by the fit to $M_{\pi^+\pi^-}$ shown in figure 1.

3.1 Fitting for R^0

We used the MINUIT [13] fitting program to perform a maximum-likelihood fit to the $M_{\pi^+\pi^-}$ shape from data, using shapes from $K_L \to \pi e\nu$, $K_L \to \pi\mu\nu$, $K_L \to \pi^+\pi^-$, $K_L \to \pi^+\pi^-\pi^0$, and $R^0 \to \pi^+\pi^-\tilde{\gamma}$ from Monte Carlo simulations. The amplitudes for all the simulated $M_{\pi^+\pi^-}$ shapes were allowed to vary independently, as was the amplitude of the trigger prescale for $M_{\pi^+\pi^-} \leq 0.45$ GeV/c^2. The agreement between data and Monte Carlo has an overall χ^2/degree of freedom of $\sim 194/148$ for the region $0.28 \text{ GeV}/c^2 \leq M_{\pi^+\pi^-} \leq 0.58 \text{ GeV}/c^2$.

Approximately 70 different R^0, $\tilde{\gamma}$ combinations were used in the fits. All fits yielded R^0 components consistent with zero. An upper limit for a given R^0 was determined by evaluating the maximum-liklihood curve at the 90% confidence interval, after shifting the peak of the curve to zero if it lay in a negative region. Table 1 lists the 90% confidence level upper limit on the number of certain R^0 found in the data, as well as the acceptance corrected number (assuming the R^0 lifetime to be equivalent to the kaon lifetime) which yields the upper limit on the number of R^0 produced at the target. The last two columns list the 90% confidence level upper limit for the R^0/K^0 flux ratio, and pQCD predicted flux ratio. Using the 2.1×10^6 $K_L \to \pi^+\pi^-$ events observed, we determined that 37.7×10^{10} K_L of all energies exited the absorbers.

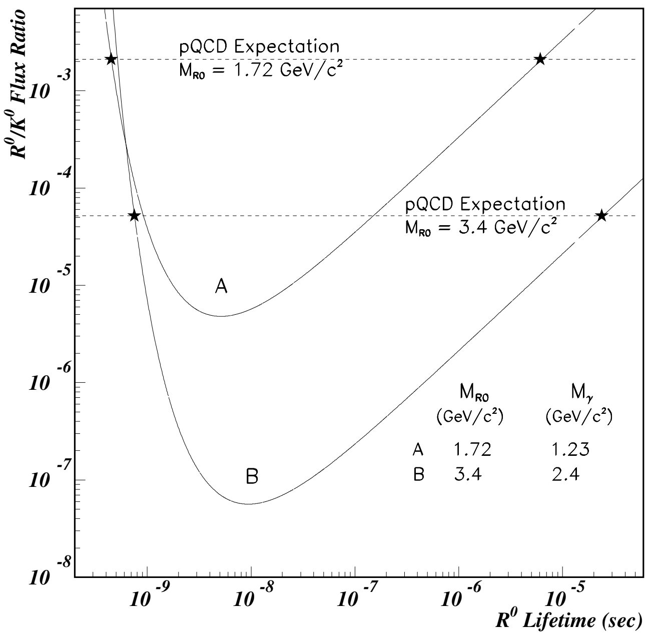

Figure 3: Upper limits with 90% confidence level on the R^0/K^0 flux ratio as a function of R^0 lifetime, for two M_{R^0}, $M_{\tilde{\gamma}}$ combinations. The dotted lines show the pQCD expectation for the flux ratio, and the stars mark the corresponding lifetime limits.

3.2 R^0 Flux Upper Limits

Figure 3 shows the variation of the 90% C.L. upper limit on the R^0/K^0 flux ratio with the R^0 lifetime for two R^0, $\tilde{\gamma}$ combinations. The dashed lines indicate the flux ratio expected due to pQCD, and the intersection of the flux prediction and limit, indicated by the stars, correspond to the lifetime limits for that particular R^0. Particles with shorter lifetimes decay too close to the target to be visible in the detector, while those with much longer lifetimes exit the detector without decaying.

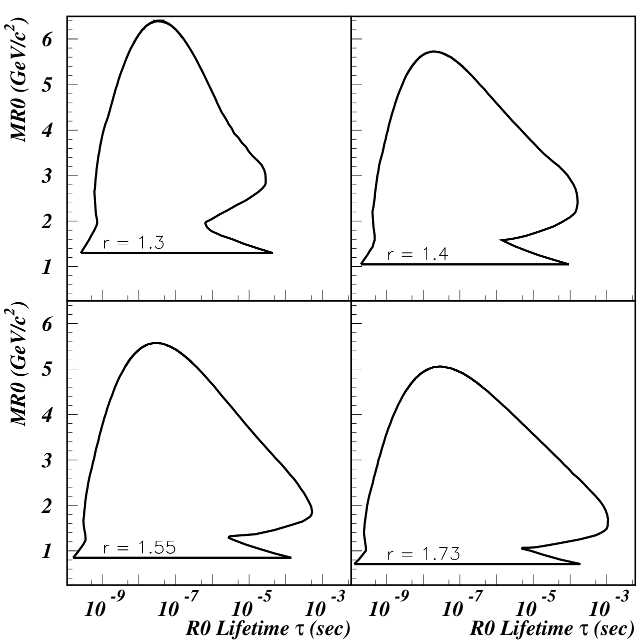

Figure 4: R^0 mass-lifetime regions excluded at 90% confidence level, assuming pQCD flux, for values of r = 1.3 (top left), 1.4 (top right), 1.55 (bottom left) and 1.73 (bottom right). The lower edges are due to the kinematic limit of $M_{R^0} - M_{\tilde{\gamma}} = 2M_\pi$.

We can now use the R^0/K^0 flux expectation from perterbative QCD to exclude a range of lifetimes for a given R^0, $\tilde{\gamma}$ combination. Figure 4 shows R^0 lifetimes excluded at 90% confidence level for a given mass. Contours are shown for r $= 1.3, 1.4, 1.55, \text{and} 1.73$.

The region of particular interest, $1.4\ \text{GeV}/c^2 \leq M_{R^0} \leq 2.2\ \text{GeV}/c^2$, is now accessible. The lower line is due to the kinematic limit of $M_{R^0} - M_{\tilde{\gamma}} = 2M_\pi$, below which the decay cannot proceed. We note that in the theoretically interesting regions of M_{R^0} and r, our exclusion covers lifetimes as low 3×10^{-10} seconds, and as high as 10^{-3} seconds.

4 Conclusion

The analysis presented in this paper excludes most R^0 masses, over six decades in lifetime. In particular the region of primary interest, $M_{R^0}/M_{\tilde{\gamma}} \leq 1.4$ and $M_{R^0} \leq 2.2\ \text{GeV/c}^2$, which was not addressed by previous direct and indirect searches, is now excluded. We thus definitively close the light gluino window. Our null result constrains most SUSY models in which gauginos remain massless at tree-level and obtain masses from loop diagrams. More generally, our understanding of the $M_{\pi^+\pi^-}$ shape will constrain many future models that require a light hadronic component in their decays.

Acknowledgements

We thank Glennys Farrar for suggesting this search and for discussions concerning this work, and along with Rocky Kolb, for pointing out the cosmological significance of this search.

References

[*] Representing the KTeV Collaboration; email: lath@physics.rutgers.edu

1. R. Mohapatra and S. Nandi, Phys. Rev. Lett. **79**, 181 (1997); Z. Chacko et al., Phys. Rev. D**56**, 5466 (1997); S. Raby, Phys. Rev. D**56**, 2852 (1997).
2. G.R. Farrar, Phys. Rev. Lett. **76**, 4111 (1996); G.R. Farrar, Phys. Rev. D **51**, 3904 (1995);
3. D.J.H. Chung, G.R. Farrar, and E.W. Kolb, Phys Rev. D **56**, 6096 (1997); G.R. Farrar and E.W. Kolb, Phys. Rev. D **53**, 2990 (1996).
4. J. Adams *et al.*, Phys Rev. Lett **79**, 4083 (1997).
5. I. Albuquerque *et al.*, Phys. Rev. Lett. **78**, 3252 (1997).
6. F. Csikor and Z. Fodor, Phys. Rev. Lett. **78**, 4335 (1997).
7. R. Barate *et al.*, Report No. CERN-PPE-97-002.
8. R.H. Bernstein *et al.*, Phys. Rev. D **37**, 3103 (1988).
9. G. R. Farrar, Nucl. Phys. Proc. Suppl. **62**, 485 (1998) (available as eprint hep-ph/9710277).
10. K. Arisaka *et al.*, Report No. FERMILAB-580-1992; L.K. Gibbons *et al.*, Phys. Rev. D **55** 6625 (1997).
11. S. Dawson, E. Eichten, and C. Quigg, Phys. Rev. D **31**, 1581 (1985).
12. C. Quigg (private communication).
13. F. James, M. Roos, Comput. Phys. Commun. **10**, 343 (1975).